Published in final edited form as:
Nat Biomed Eng. 2017 January ; 1(1): . doi:10.1038/s41551-016-0005.

Self-adjusting synthetic gene circuit for correcting insulin resistance

Haifeng Ye[#1,2,*], **Mingqi Xie**[#1], **Shuai Xue**[2], **Ghislaine Charpin-El Hamri**[3], **Jianli Yin**[2], **Henryk Zulewski**[1,4,5], and **Martin Fussenegger**[1,6,*]

[1]Department of Biosystems Science and Engineering, ETH Zurich, Mattenstrasse 26, CH-4058 Basel, Switzerland [2]Shanghai Key Laboratory of Regulatory Biology, Institute of Biomedical Sciences and School of Life Sciences, East China Normal University, Dongchuan Road 500, 200241 Shanghai, China [3]Institut Universitaire de Technologie, IUT, Département Génie Biologique, F-69622 Villeurbanne Cedex, France [4]Division of Endocrinology, Diabetes and Metabolism, University Hospital Basel, Petersgraben 4, CH-4031 Basel, Switzerland [6]University of Basel, Faculty of Science, Mattenstrasse 26, CH-4058 Basel, Switzerland

[#] These authors contributed equally to this work.

Abstract

By using tools from synthetic biology, sophisticated genetic devices can be assembled to reprogram mammalian cell activities. Here, we demonstrate that a self-adjusting synthetic gene circuit can be designed to sense and reverse the insulin-resistance syndrome in different mouse models. By functionally rewiring the mitogen-activated protein kinase (MAPK) signalling pathway to produce MAPK-mediated activation of the hybrid transcription factor TetR-ELK1, we assembled a synthetic insulin-sensitive transcription-control device that self-sufficiently distinguished between physiological and increased blood insulin levels and correspondingly fine-tuned the reversible expression of therapeutic transgenes from synthetic TetR-ELK1-specific promoters. In acute experimental hyperinsulinemia, the synthetic insulin-sensing designer circuit reversed the insulin-resistance syndrome by coordinating expression of the insulin-sensitizing compound adiponectin. Engineering synthetic gene circuits to sense pathologic markers and coordinate the expression of therapeutic transgenes may provide opportunities for future gene- and cell-based treatments of multifactorial metabolic disorders.

[*]To whom correspondence should be addressed: M.F. (Tel: +41 61 387 31 60, Fax: +41 61 387 3988, fussenegger@bsse.ethz.ch) or H.Y. (Tel: +86 21 5434 1058, Fax: +86 21 5434 2908, hfye@bio.ecnu.edu.cn).
[5]Present address: Division of Endocrinology and Diabetes, Stadtspital Triemli, Birmensdorferstrasse 497, CH-8063 Zurich, Switzerland.

Author contributions

H.Y., M.X., H.Z. and M.F. designed the project, analysed the results and wrote the manuscript. H.Y., M.X., G.H.E., S.X., and J.Y. performed the experimental work.

Competing financial interests

The authors declare no competing financial interests.

Europe PMC Funders Author Manuscripts

Europe PMC Funders Author Manuscripts

Over the past decades obesity has resulted in an epidemic prevalence of type 2 diabetes, affecting more than 400 million individuals worldwide1. Obesity-induced insulin resistance results from complex metabolic and inflammatory changes and is the key etiologic defect of the metabolic syndrome, a cluster of clinical findings including hypertension and dyslipidaemia increasing the imminence of cardiovascular disorders and type 2 diabetes2,3. The physiological response to insulin resistance and impaired glucose metabolism is the continuous stimulation of insulin secretion, which initiates the gradual decline of pancreatic beta cells thereby leading to progressive development of type-2 diabetes and its acute and chronic complications4. Current insulin-resistance therapies focusing on the reduction of body weight or the administration of insulin-sensitising drugs such as Glitazones were ineffective or associated with important side effects2,5–7. Insulin resistance is inversely correlated with blood levels of adiponectin8–10, the most abundant adipose tissue-derived hormone with insulin-sensitizing properties11. Therefore, the development of drugs that increase blood adiponectin levels are currently in the limelight for the treatment of insulin resistance and the associated cardiovascular risk factors10.

Synthetic biology, the engineering science of reassembling standardized biological parts in a systematic, rational and predictable manner to program novel cellular behaviour, has enabled the design of synthetic gene networks that can synchronize early diagnosis of a pathologic situation with targeted therapeutic intervention in a closed-loop control manner12. For example, designer-cell implants with embedded therapeutic gene networks have been successfully used to diagnose, prevent and cure experimental diseases13. Therefore, synthetic biology-inspired therapeutic strategies14–18 may provide new treatment opportunities to mitigate insulin resistance. We have designed and engineered a mammalian synthetic sensor-effector device that is exclusively activated by high insulin levels and triggers corresponding expression of adiponectin, which reverses insulin resistance and its related metabolic effects by restoring glucose and lipid homeostasis in different mouse models covering various stages of insulin resistance (Fig. 1a).

Design of the synthetic insulin-sensor device

The insulin-sensor device was designed by engineering mammalian cells for ectopic expression of the human insulin receptor19,20 and rewiring its native signalling cascade involving the IRS-1-Ras-MAPK pathway21 to the synthetic hybrid transcription factor, TetR-ELK122. The activation of the MAPK kinase phosphorylates TetR-ELK1, rendering it a potent transactivator that triggers transcription from synthetic promoters containing multiple TetR-ELK1-binding sites. In addition, the insulin-triggered transgene expression circuit is not only regulated by the phosphorylation status of the ELK1-domain; the operator-binding affinity of the TetR moiety can also be inhibited by administration of the antibiotic doxycycline. Thus, TetR-ELK1 represents a dual-input transcription factor which interfaces insulin levels with therapeutic transgene expression and provides a safety latch to modulate or switch off the device by a clinically licensed antibiotic (Fig. 1b). Western blot analyses involving probing IR, phospho-IRS-1 and phospho-ERK signals confirmed that HEK-293 cells transfected with the human insulin receptor-encoding expression vector pIR (P_{hCMV}-IR-pA) and incubated with insulin indeed activated the IRS-1-Ras-MAPK signalling pathway (Supplementary Fig. 1a,c,e). HEK-293 cells were co-transfected with a

constitutive human insulin receptor-encoding expression vector, pIR (P_{hCMV}-IR-pA); a constitutively expressed hybrid transcription factor TetR-ELK1 (pTetR-ELK1; P_{hCMV}-TetR-ELK1-pA); and a phosphorylated TetR-ELK1-dependent, $P_{hCMV*-1}$-driven human placental secreted alkaline phosphatase (SEAP) reporter construct, pMF111 ($P_{hCMV*-1}$-SEAP-pA). As a result, although Western blot analyses showed the presence of endogenous IR and associated signalling cascade (Supplementary Fig. 1b,d,f), SEAP was exclusively induced in the cells transfected with the human insulin receptor but not in control cells expressing either the fluorescent reporter gene EYFP or the unrelated chimeric trace-amine-associated receptor 1 (cTAAR1) (Supplementary Fig. 2). This finding confirmed that HEK-293 cells engineered with the insulin-sensor device could be specifically activated by insulin. Insulin-inducible transgene expression was functional in different pIR-/pTetR-ELK1-/pMF111-co-transfected mammalian cell lines, suggesting that this synthetic insulin-sensor device is broadly applicable as a mammalian gene switch (Fig. 2a). However, possible differences in the availability and compatibility of the endogenous signal transduction components with insulin-triggered human insulin receptor-mediated input resulted in a wide range of induction profiles between different cell lines (Fig. 2a). Because HEK-293 cells exhibited the best insulin-triggered transgene expression profile, they were used in all of the following studies.

Validation of the synthetic insulin-sensor device

To evaluate the adjustability of the insulin-triggered transgene expression, pIR-/pTetR-ELK1-/pMF111-engineered HEK-293 cells were incubated with increasing insulin doses, and the SEAP levels were profiled every 24 hours for up to 3 days (Fig. 2b). The SEAP levels correlated precisely with increasing insulin doses up to 20 ng/mL and exhibited reliable induction levels over the entire concentration range (Fig. 2b). When the engineered cells were exposed to high doses of 20 ng/mL insulin for various time periods, the SEAP production kinetics could be precisely programmed (Fig. 2c). Similar insulin-triggered expression kinetics were also visualised by fluorescence microscopy in cells engineered with pHY74 ($P_{hCMV*-1}$-EYFP-pA) instead of pMF111 (Fig. 2d). The product gene expression levels could be reliably switched ON and OFF by alternating the presence and absence of insulin in the culture medium, demonstrating that this synthetic insulin-sensor device was fully reversible *in vitro* (Fig. 2e) and *in vivo* (Supplementary Fig. 3). Moreover, the insulin-triggered transgene expression levels could be dose- and time-dependently modulated by doxycycline (Fig. 2f), and the original levels could be fully recovered simply by the removal of doxycycline (Fig. 2g). Therefore, transgene expression by this insulin-sensor device was not only positively regulated by the addition of insulin; it could also be negatively adjusted by the administration of doxycycline, which functioned as a safety latch to flexibly terminate transgene expression during any undesired scenarios. More importantly, further control experiments showed that the engineered insulin-sensor device was specific for insulin (Supplementary Fig. 3) and insensitive to glucose (Supplementary Fig. 4 and Supplementary Fig. 5), which insulates the insulin-sensor device from insulin-controlled glucose metabolism.

Sensitivity of the insulin-sensor device

Next, we evaluated whether the synthetic insulin-sensor device could sense high insulin concentrations and trigger transgene expression both *in vitro* and *in vivo*. To demonstrate the diagnostic capacity of the synthetic insulin-sensor device *in vitro*, pIR-/pTetR-ELK1-/pMF111-engineered HEK-293 cells were incubated with 10% serum from three different mouse models of insulin resistance (ob/ob, db/db, DIO). The SEAP levels were profiled after 72 hours (Supplementary Fig. 6a), which confirmed that the serum containing high levels of insulin (Supplementary Fig. 6b) from insulin-resistant mice could trigger transgene expression in insulin-sensor cells. Similarly, serum from human patients who developed obesity-induced insulin resistance could also trigger the SEAP expression (Supplementary Fig. 6c,d). To validate insulin-triggered transgene expression *in vivo*, $2x10^6$ microencapsulated pIR-/pTetR-ELK1-/pMF111-transgenic HEK-293 cells were intraperitoneally implanted into three different mouse models: mice with insulin-resistant diabetes due to leptin (ob/ob mice) or leptin receptor (db/db mice) deficiency and diet-induced obesity (DIO), all of which develop hyperinsulinemia. Control animals were implanted with pKZY73 (P_{SV40}-cTAAR1-pA)-/pTetR-ELK1-/pMF111-transgenic HEK-293 cells. The corresponding serum SEAP levels of the treated mice were profiled after 48 hours (Supplementary Fig. 7a-c), which confirmed that the synthetic insulin-sensor circuit could sense high insulin concentrations (from 5-20 ng/mL) in insulin-resistant ob/ob, db/db, and DIO mouse models.

Closed-loop adiponectin expression in ob/ob mice

To convert the diagnostic insulin-sensor device into a self-sensing therapeutic cell implant that automatically detects and treats insulin resistance, we linked the hyperinsulinemia input to the expression of adiponectin (Supplementary Fig. 8) and implanted microencapsulated pIR-/pTetR-ELK1-/pHY79 ($P_{hCMV*-1}$-Fc-adiponectin-pA)-transgenic HEK-293 cells into the peritoneum of insulin-resistant ob/ob mice. Adiponectin can reverse obesity-induced insulin resistance by improving insulin sensitivity and decreasing the lipid content in the body[21, 22] and the Fc-adiponectin derivative was selected based on improved half-life and therapeutic efficacy[23]. After 48 hours of implantation, the ob/ob mice containing transgenic cell implants exhibited significantly increased serum adiponectin levels (Fig. 3a). Within 48 hours, the increased adiponectin levels significantly lowered free fatty acid, cholesterol and insulin levels in the insulin-resistant ob/ob mice (Fig. 3b-d). Within 24 h, increased adiponectin levels (1.56±0.23nM) attenuated glycaemic excursions in response to intraperitoneal glucose tolerance tests (Fig. 3e) and increased insulin sensitivity in response to intraperitoneal insulin tolerance tests (Fig. 3f). Homeostatic model assessment-estimated insulin resistance (HOMA-IR[24,25]) revealed that insulin resistance significantly decreased during the treatment (Fig. 3g). Additionally, decreased food intake (Fig. 3h) and body weight (Fig. 3i) could also be observed 3 days after implantation. These results suggest that the synthetic insulin-sensor circuit was sufficiently sensitive to alleviate the insulin resistance syndrome and may be suitable for the treatment of obesity-induced insulin resistance.

Closed-loop adiponectin expression in DIO mice

The synthetic insulin-sensor circuit was also evaluated for the treatment of DIO mice, which are insulin-resistant and develop prediabetic obesity. As above, we implanted $2x10^6$ microencapsulated pIR-/pTetR-ELK1-/pHY79-transgenic HEK-293 cells intraperitoneally into DIO or wild-type mice. After 48 hours of implantation, the DIO mice containing the transgenic cell implants showed significantly elevated blood adiponectin levels (Fig. 4a). Within 48 hours, the increased adiponectin levels significantly lowered free fatty acid, cholesterol and insulin levels in the insulin-resistant DIO mice (Fig. 4b-d). Within 24 h increased adiponectin levels (1.38±0.18nM) attenuated glycaemic excursions in response to intraperitoneal glucose tolerance tests (Fig. 4e) and increased insulin sensitivity in response to intraperitoneal insulin tolerance tests (Fig. 4f). HOMA-IR values indicated that insulin resistance significantly decreased during the treatment (Fig. 4g). Additionally, decreased food intake (Fig. 4h) and body weight (Fig. 4i) could also be observed 3 days after implantation. These results further confirmed that the synthetic insulin-sensor circuit is also applicable for the treatment of prediabetic insulin resistance syndromes such as diet-induced obesity.

Self-sufficient long-term correction of insulin-resistance

To confirm the long-term therapeutic efficacy of the synthetic insulin-sensor device, we have produced the clonal cell line $HEK_{IR\text{-}Adipo}$ which is stably transgenic for pHY118 (ITR-$P_{hCMV*\text{-}1}$-Fc-adiponectin-P2A-EGFP-pA:P_{mPGK}-PuroR-pA-ITR) and pHY121 (ITR-P_{hCMV}-IR-P2A-TetR-Elk1-pA:P_{mPGK}-ZeoR-pA-ITR). After implantation of microencapsulated $HEK_{IR\text{-}Adipo}$ cells into ob/ob (Fig. 5) and DIO mice (Fig. 6), $HEK_{IR\text{-}Adipo}$ self-sufficiently detected hyperinsulinemia and produced, secreted and systemically delivered adiponectin (Figs. 5a, 6a) which substantially decreased blood insulin levels (Figs. 5b, 6b) as well as serum lipids (Figs. 5c,d, 6c,d), insulin resistance (Figs. 5e, 6e), food intake (Figs. 5f, 6f) and body weight (Fig. 5g, 6g). Interestingly, the control performance of the synthetic insulin-sensor device in a stable clonal context ($HEK_{IR\text{-}Adipo}$) was almost identical when compared to transiently transfected circuit-transgenic HEK-293 cells during the first 72h after implantation, but $HEK_{IR\text{-}Adipo}$ showed superior treatment efficacy in long-term experiments (Fig. 5 and Fig. 6).

Discussion

Insulin resistance is the hallmark the metabolic syndrome that has a complex multifactorial aetiology; it is primarily induced by visceral obesity and can trigger the initiation of type 2 diabetes and atherosclerotic vascular disease2,26. Decreased adiponectin signalling appears to play a central role in the process and represent an attractive treatment target8–11. Recently, synthetic biology has substantially advanced the design of biomedical circuits, providing new therapeutic strategies14,27–31. Synthetic biology-inspired gene- and cell-based therapies may provide new opportunities in the treatment of insulin-resistance-related metabolic disorders.

By functionally assembling a human insulin receptor and control modules (TetR-ELK1, $P_{hCMV*-1}$) with native intracellular machineries (the IRS-1-Ras-MAPK signalling cascade), we rewired the insulin receptor-mediated tyrosine kinase-coupled receptor signalling pathway to a synthetic hybrid TetR-ELK1 transcription factor by utilising their common intracellular MAPK-based signalling system as the interface. We have designed the insulin-sensor-controlled expression of the half-life-optimised version of adiponectin23 that enables (i) the constant monitoring of insulin levels in the blood; (ii) the automatic activation of the sensor device in response to high insulin levels, (iii) the coordinated production of adiponectin, which promptly reduced blood glucose, free fatty acid, cholesterol and HOMA-IR levels in insulin-resistant ob/ob and DIO mice, and (iv) self-sufficiently reached adiponectin homeostasis based on closed-loop control to reduce the risk of potential adiponectin-related side effects.

Adiponectin acts on various peripheral tissues as well as the central nervous system and has been associated with a wide variety of therapeutic effects including anti-inflammatory activities, insulin sensitization, anti-atherogenesis as well as reduction of blood-fat levels, food intake and body weight32. This multifaceted role of adiponectin makes a precise prediction of its therapeutic impact and potential side effects challenging. Therefore, dosing of adiponectin may be of particular importance as long-term high-dose administration of adiponectin could cause some adverse effects. The closed-loop topology of the insulin-sensor device managing self-adjusting adiponectin production in response to the state of insulin resistance is expected to prevent adiponectin overdosing.

The synthetic signalling cascade of the insulin-sensor device contains the chimeric transcription factor TetR-ELK1 which provides a non-limiting example for an additional layer of control using the clinically licensed antibiotic doxycycline33. Although antibiotic-triggered interventions were not required to trim the insulin-sensor device to correct experimental insulin resistance, orthogonal remote control may become important in future clinical applications to tune, adapt and adjust adiponectin expression to the optimal patient-specific therapeutic window and provide emergency interventions to inactivate the device in case of complications.

The current insulin-sensor device has been engineered into HEK-293 cells but future clinical applications may require autologous parental cells such as the patients' own mesenchymal stem cells which have already been clinically validated34. No matter which cell type will prevail in future therapies, the designated treatment strategy remains identical: (i) large-scale manufacturing of patient-specific designer cells, (ii) frozen storage of the designer cells either before or after (iii) encapsulation inside a vascularising immunoprotective container35, (iv) implantation of the encapsulated designer cells preferably subcutaneously where (v) they can easily be replaced at regular intervals by a minimal ambulant intervention in the event of fibrosis.

Outlook

The insulin-sensor/effector device was able to substantially improve insulin resistance and the associated metabolic dysfunctions in different mouse models exhibiting various features

of the metabolic syndrome similar to that observed in humans. This designer circuit performed as expected and has the potential as a therapeutic tool for treatment of early stages of diabetes mellitus in future clinical applications. Self-sufficient synthetic gene circuits could become of clinical relevance in the not-too-distant future in the treatment of multifactorial metabolic disorders in which the presence of specific disease markers can be rapidly and specifically detected and for which the expression of a suitable therapeutic protein can be immediately coordinated.

Because therapeutic gene circuits designed in this manner most efficiently coordinate disease marker monitoring with disease modulating molecular interventions for a particular disorder, developing and optimising biologically safe implants harbouring designer cells transgenic for those rationally designed circuits would be an important breakthrough and may represent a new era in modern molecular personalized medicine.

Methods

Vector design

Comprehensive design and construction details for all expression vectors are listed in Table S1. Some expression vectors were constructed by Gibson assembly using the GeneArt® Seamless Assembly Cloning Kit (Obio Technology, Shanghai, China; cat. no.BACR(C)20144001). All constructs were confirmed by sequencing (Genewiz Inc., Suzhou, China).

Cell culture and transfection

Human embryonic kidney cells (HEK-293, ATCC: CRL-11268), human cervical adenocarcinoma cells (HeLa, ATCC: CCL-2) and human bone marrow stromal cells (hMSCs) immortalised by the expression of the human telomerase catalytic subunit (hTERT; hMSC-TERT)36 were cultured in Dulbecco's modified Eagle's medium (DMEM, Invitrogen) supplemented with 10% (vol/vol) fetal calf serum (FCS; cat. no. 201F10, lot no. PE01026P, BioConcept, Allschwil, Switzerland) and 1% (vol/vol) penicillin/streptomycin solution (Biowest, Nuaillé, France; cat. no. L0022-100, lot no. S09965L0022). Chinese hamster ovary cells (CHO-K1, ATCC: CCL-61) were cultivated in ChoMaster® HTS (Cell Culture Technologies, Gravesano, Switzerland) supplemented with 5% (vol/vol) FCS and 1% (vol/vol) penicillin/streptomycin solution. All of the cell types were cultivated at 37°C in a humidified atmosphere containing 5% CO_2 and were regularly tested for the absence of *Mycoplasma* and bacterial contamination. HEK-293, HeLa, hMSC-TERT and CHO-K1 cells were (co-)transfected using an optimised polyethyleneimine (PEI)-based protocol37 In brief, $5x10^4$ cells per well were seeded per well of a 24-well plate and (co-)transfected with a total of 0.6μg of plasmid DNA mixture (for the cotransfections, a 1:1:1 receptor/processor/reporter plasmid ratio was used) diluted in 25μL of FCS-free DMEM solution and subsequently mixed with 25μL polyethyleneimine solution containing 1.8μL of polyethyleneimine (1mg/mL in ddH_2O; Polysciences, Eppelheim, Germany; cat. no. 24765-2) diluted in FCS-free DMEM. The DNA-PEI mixture solution was incubated for 15 min at 22°C and added dropwise to the cells. After a 6-h (co-)transfection, the medium was replaced. For the mouse experiment, $7x10^6$ HEK-293 cells were seeded into a 15-cm cell

culture dish and (co-)transfected with a total of 30μg of plasmid DNA mixture (a 1:1:1 receptor/processor/reporter plasmid ratio was used) diluted in 1500μL of FCS-free DMEM solution, and then, the cells were subsequently mixed with 1500μL polyethyleneimine solution containing 90μL of polyethyleneimine (1mg/mL in ddH_2O) diluted in FCS-free DMEM. After 15 min of incubation at 22°C, the DNA-PEI mixture was added dropwise to the cells, and the cells were harvested for encapsulation after 6h of transfection.

Generation of stable cell lines

The $HEK_{IR\text{-}Adipo}$ cell line, transgenic for insulin-triggered Fc-adiponectin and EGFP expression, was constructed by co-transfecting $5x10^4$ HEK-293 cells with 135ng of pHY118 (ITR-$P_{hCMV*\text{-}1}$-Fc-adiponectin-P2A- EGFP-pA:P_{mPGK}-PuroR-pA-ITR), 135ng of pHY121 (ITR-P_{hCMV}-IR-P2A-TetR-Elk1-pA: P_{mPGK}-ZeoR-pA-ITR), and 30ng Sleeping Beauty transposase expression vector pCMV-T7-SB10038 (PhCMV-SB100X-pA). After cultivation with 1μg/mL puromycin and 100μg/mL zeocin for two weeks, the $HEK_{IR\text{-}Adipo}$ cell line was selected based on green-fluorescence intensity by FACS-mediated cell sorting using a Becton Dickinson FACSAria™ Cell Sorter (BD Biosciences, San Jose, CA, USA).

Reporter gene assays

The production of human placental SEAP was quantified in cell culture supernatants39 and mouse serum40 as described previously. EYFP expression was visualised using a LEICA DMI-600 microscope (Leica Microsystems, Heerbrugg, Switzerland) equipped with a DFC350FX R2 digital camera (Leica), a 10x objective, a 488 nm/509 nm (B/G/R) excitation/emission filter set and Leica Application Suite software (version V2.1.0R1).

Western blot analysis

To analyze the IRS-1-Ras-MAPK signaling cascade activation through the human insulin receptor, HEK-293 cells were cotransfected with pIR, pTetR-ELK1 and pMF111. After 48h of transfection, the cells were starved for 6h, and then, 0-20ng/mL insulin was added to the cells. After 1h of insulin stimulation, $2x10^6$ HEK-293 cells were collected, and protein extracts were prepared as described previously41,42. The proteins were resolved on a 12% SDS polyacrylamide gel and electroblotted onto a polyvinylidene fluoride (PVDF) membrane (Immobilon®-P, Millipore, Billerica, MA, USA). Phospho-Erk1/2 was visualised using a primary rabbit polyclonal anti-phospho-p44/42 MAPK (Erk1/2) (Thr202/Tyr204) antibody (Cell Signaling, BioConcept, Allschwil, Switzerland; cat. no. 4370, lot no. 12) and a secondary DyLight® 800-labeled goat anti-rabbit IgG (KPL, USA; cat. no. 072-07-16-06, lot no. 130561). ERK1/2 was visualised using a primary rabbit p44/p42 MAPK (ERK1/2) antibody (Cell Signaling, Danvers, USA; cat. no. 4695, lot no. 14) and the secondary DyLight® 800-labeled goat anti-rabbit IgG. IR was visualized using an insulin receptor-specific primary rabbit monoclonal antibody (Abcam, Cambridge, MA, USA; cat. no. 131238, lot. no. GR219882-1) and the DyLight® 800-labeled goat anti-rabbit IgG. Phospho-IRS-1 was visualized using a phospho-IRS-1-specific primary rabbit monoclonal antibody (Abcam, Cambridge, MA, USA; cat. no. ab46800, lot. no. GR98847-17) and the secondary DyLight® 800-labeled goat anti-rabbit IgG. β-actin was visualized using a β-actin-specific primary mouse monoclonal antibody (Sigma-Aldrich, Saint Louis, MO, USA; cat. no. A5441, lot. no. 122m4782) and a secondary DyLight® 800-labeled goat anti-mouse IgG

(ThermoFisher Scientific, Shanghai, China; cat. no. SA5-10176, lot no. 130561). All proteins were detected using the Odyssey system (LI-COR Biosciences, Lincoln, NE, USA).

Animal experiments

Intraperitoneal implants were produced by encapsulating transgenic HEK-293 cells into coherent alginate-poly-(L-lysine)-alginate beads (400μm; 200 cells/capsule) using an Inotech Encapsulator Research Unit IE-50R (EncapBioSystems Inc., Greifensee, Switzerland) set to the following parameters: a 200-μm nozzle with a vibration frequency of 1025Hz, a 25-mL syringe operated at a flow rate of 410 units and 1.12-kV voltage for bead dispersion. DIO mice were developed for the mouse studies. Typically, four-week-old male C57BL/6J mice (Charles River Laboratory) were fed a high-fat diet (60% kcal, D12492, Research Diets Inc., New Brunswick, NJ, USA) for 10 weeks; thus, these mice became obese, hyperglycaemic and insulin resistant. Control mice were fed a low-fat control diet (10% kcal, D12450J, Research Diets Inc.) for 10 weeks. Type 1 diabetic mice were developed for the study of the tunability of insulin-sensor device in mice. Eight week-old wild-type male C57BL/6J mice were used to create diabetes models. Mice after 16 hours fast were intraperitoneally injected with streptozotocin (60mg/kg of body weight, Sigma-Aldrich, USA, cat. no. S0130) in 0.1M citrate buffer daily for 6 days. Only animals with blood glucose levels above 250mg/dl were used in the study. Twelve-week-old male insulin-resistant db/db (BKS.Cg-Dock7^{m} +/+ Lepr^{db}/J, derived from C57BL/6J mice, Charles River Laboratory), ob/ob (B6.V-Lep^{ob}/J, derived from C57BL/6J mice, Charles River Laboratory), DIO and wild-type control mice (C57BL/6J, Charles River Laboratory) were intraperitoneally injected with 800μL of DMEM containing 2x10^{6} encapsulated pIR-/pTetR-ELK1-/pMF111-transgenic HEK-293 cells (200 cells/capsule). The control groups of mice received 2x10^{6} encapsulated pKZY73 (cTAAR1)-/pTetR-ELK1-/pMF111-transgenic HEK-293 cells. Blood samples were collected 48h after implantation, and the SEAP levels were quantified in the serum, which was isolated using microcontainer SST tubes according to the manufacturer's instructions (Becton Dickinson, Allschwil, Switzerland). To assess the therapeutic potential of insulin-triggered adiponectin expression in mouse models of insulin resistance (ob/ob, DIO), 12-week-old male mice were intraperitoneally implanted with 2x10^{6} microencapsulated pIR-/pTetR-ELK1-/pHY73- or pIR-/pTetR-ELK1-/pHY79-transgenic HEK-293 cells (200 cells/capsule). After two days of implantation, the treated animals were fasted for 4 hours (unless otherwise indicated) to profile their blood levels of glucose (using a glucometer; Contour, Bayer HealthCare, Basel Switzerland), insulin (mouse insulin ELISA kit; Mercodia, Uppsala, Sweden; cat. no. 10-1247-01), hIgG1-Fc-Adiponectin (human IgG ELISA kit; Immunology Consultants Laboratory Inc., Portland, OR; cat. no. E-80G), free fatty acids (NEFA-HR2 kits; Wako Chemical GmbH, Neuss, Germany; cat. nos. 999-34691; 995-34791; 991-34891; 993-35191; 276-76491), and cholesterol (LabAssay Cholesterol kit; Wako Chemical GmbH, Neuss, Germany; cat. no. 439-17501). Homeostatic model-assessment-estimated insulin resistance (HOMA-IR) was determined according to a standard formula24. For glucose-tolerance tests, mice were fasted for 16h before they received an intraperitoneal injection of 1.5 g/kg D-glucose in ddH_2O, and the glycaemic profile of each animal was tracked every 30min for up to 2h. For insulin-tolerance tests, mice were fasted for 4h before they received an intraperitoneal injection of

Europe PMC Funders Author Manuscripts

1U/kg recombinant insulin (Sigma-Aldrich, Saint Louis, MO, USA; cat. no. I3536), and the glycaemic profile of each animal was tracked every 30min for up to 2h.

All experiments involving animals were performed according to the directives of the European Community Council (2010/63/EU), approved by the French Republic (69266310) and performed by G.C.-E.H. at the University of Lyon, Institut Universitaire de Technologie (IUTA), F 69622 Villeurbanne Cedex, France, and also approved by the East China Normal University (ECNU) Animal Care and Use Committee and in direct accordance with the Ministry of Science and Technology of the People's Republic of China on Animal Care guidelines. The protocol was approved by ECNU Animal Care and Use Committee (Protocol ID: m20140707).

Human blood samples

All the experiments involving human blood samples were approved by the Ethics Committee of the ETH Zurich (EK 2012-N-42). Whole blood from healthy and obese individuals was collected using standard venous blood-collection tubes and serum was prepared according to the manufacturer's instructions (BD Vacutainer, Becton Dickinson AG, Allschwil, Switzerland; cat. no. 366480). Serum insulin levels were quantified using a human insulin ELISA kit (Mercodia, Uppsala, Sweden; cat. no. 10-1113-01).

Statistical analyses

All *in-vitro* data represent the mean ± SD of three independent experiments (n=3). For animal experiments, each treatment group consists of eight mice randomly selected from the same delivered pool with the particular genetic background (n=8). Blood sample analysis was blinded. After assessing normality assumptions and group standard deviations, a Student’s *t*-test was considered more appropriate than non-parametric group comparison statistics such as the Wilcoxon rank-sum test. Therefore, all group comparisons were analysed by the Student’s *t*-test (cut-off of $P < 0.05$) using GraphPad Prism 6 software (GraphPad Softwarew Inc., La Jolla, CA).

Data availability

The authors declare that all data supporting the findings of this study are available within the paper and its supplementary information files. Sequence information of key components is available at GenBank: human insulin receptor hIR, GenBank ID: BC117172.1; Synthetic hybrid transcription factor TetR-ELK1, GenBank ID: KY053478; Custom-designed Fc-adiponectin, GenBank ID: KY053479.

Supplementary Material

Refer to Web version on PubMed Central for supplementary material.

Acknowledgements

We thank Ted Abel for providing the pTetR-ELK1 (MKp37) plasmid, Barbara Geering for providing human serum from healthy individuals, Yuping Lai for providing the DyLight® 800-labeled goat anti-mouse IgG, Brian M. Lang as well as Leo Scheller for assistance with the statistical analyses and Marie Daoud El Baba for skilful assistance with the animal study. This work was supported by a European Research Council (ERC) advanced grant (No.

321381) and in part, by the Cantons of Basel and the Swiss Confederation within the INTERREG IV A.20 trinational research program as well as by the Gutenberg Chair awarded to M.F. This work was also supported by the National Key Research and Development Program of China, Stem Cell and Translational Research (No. 2016YFA0100300), by the National Natural Science Foundation of China (NSFC; No. 31470834, No. 31522017, No. 31670869), by the Science and Technology Commission of Shanghai Municipality (No. 15QA1401500, No. 14JC1401700), and Thousand Youth Talents Plan to H.Y.

References

1. Worldwide trends in diabetes since 1980: a pooled analysis of 751 population-based studies with 4.4 million participants. Lancet. 2016; 387:1513–1530. DOI: 10.1016/S0140-6736(16)00618-8 [PubMed: 27061677]
2. Johnson AM, Olefsky JM. The origins and drivers of insulin resistance. Cell. 2013; 152:673–684. DOI: 10.1016/j.cell.2013.01.041 [PubMed: 23415219]
3. Samuel VT, Shulman GI. Mechanisms for insulin resistance: common threads and missing links. Cell. 2012; 148:852–871. DOI: 10.1016/j.cell.2012.02.017 [PubMed: 22385956]
4. Prentki M, Nolan CJ. Islet beta cell failure in type 2 diabetes. The Journal of clinical investigation. 2006; 116:1802–1812. DOI: 10.1172/JCI29103 [PubMed: 16823478]
5. Christensen R, Kristensen PK, Bartels EM, Bliddal H, Astrup A. Efficacy and safety of the weight-loss drug rimonabant: a meta-analysis of randomised trials. Lancet. 2007; 370:1706–1713. DOI: 10.1016/S0140-6736(07)61721-8 [PubMed: 18022033]
6. Gloy VL, et al. Bariatric surgery versus non-surgical treatment for obesity: a systematic review and meta-analysis of randomised controlled trials. BMJ. 2013; 347:f5934.doi: 10.1136/bmj.f5934 [PubMed: 24149519]
7. Loke YK, Kwok CS, Singh S. Comparative cardiovascular effects of thiazolidinediones: systematic review and meta-analysis of observational studies. BMJ. 2011; 342:d1309.doi: 10.1136/bmj.d1309 [PubMed: 21415101]
8. Weyer C, et al. Hypoadiponectinemia in obesity and type 2 diabetes: close association with insulin resistance and hyperinsulinemia. J Clin Endocrinol Metab. 2001; 86:1930–1935. DOI: 10.1210/jcem.86.5.7463 [PubMed: 11344187]
9. Gao H, et al. Evidence of a causal relationship between adiponectin levels and insulin sensitivity: a Mendelian randomization study. Diabetes. 2013; 62:1338–1344. DOI: 10.2337/db12-0935 [PubMed: 23274890]
10. Li S, Shin HJ, Ding EL, van Dam RM. Adiponectin levels and risk of type 2 diabetes: a systematic review and meta-analysis. JAMA. 2009; 302:179–188. DOI: 10.1001/jama.2009.976 [PubMed: 19584347]
11. Ziemke F, Mantzoros CS. Adiponectin in insulin resistance: lessons from translational research. Am J Clin Nutr. 2010; 91:258S–261S. DOI: 10.3945/ajcn.2009.28449C [PubMed: 19906806]
12. Slomovic S, Pardee K, Collins JJ. Synthetic biology devices for in vitro and in vivo diagnostics. Proceedings of the National Academy of Sciences of the United States of America. 2015; 112:14429–14435. DOI: 10.1073/pnas.1508521112 [PubMed: 26598662]
13. Bai P, et al. A synthetic biology-based device prevents liver injury in mice. J Hepatol. 2016; 65:84–94. DOI: 10.1016/j.jhep.2016.03.020 [PubMed: 27067456]
14. Ye H, Aubel D, Fussenegger M. Synthetic mammalian gene circuits for biomedical applications. Current opinion in chemical biology. 2013; 17:910–917. [PubMed: 24466575]
15. Bacchus W, Aubel D, Fussenegger M. Biomedically relevant circuit-design strategies in mammalian synthetic biology. Molecular systems biology. 2013; 9:691.doi: 10.1038/msb.2013.48 [PubMed: 24061539]
16. Ye H, et al. Pharmaceutically controlled designer circuit for the treatment of the metabolic syndrome. Proceedings of the National Academy of Sciences of the United States of America. 2013; 110:141–146. DOI: 10.1073/pnas.1216801110 [PubMed: 23248313]
17. Kim T, Folcher M, Doaud-El Baba M, Fussenegger M. A synthetic erectile optogenetic stimulator enabling blue-light-inducible penile erection. Angewandte Chemie. 2015; 54:5933–5938. DOI: 10.1002/anie.201412204 [PubMed: 25788334]

18. Auslander D, et al. A synthetic multifunctional mammalian pH sensor and CO2 transgene-control device. Molecular cell. 2014; 55:397–408. DOI: 10.1016/j.molcel.2014.06.007 [PubMed: 25018017]
19. Jacob KK, Whittaker J, Stanley FM. Insulin receptor tyrosine kinase activity and phosphorylation of tyrosines 1162 and 1163 are required for insulin-increased prolactin gene expression. Mol Cell Endocrinol. 2002; 186:7–16. [PubMed: 11850117]
20. Siddle K. Signalling by insulin and IGF receptors: supporting acts and new players. J Mol Endocrinol. 2011; 47:R1–10. DOI: 10.1530/JME-11-0022 [PubMed: 21498522]
21. Altarejos JY, Montminy M. CREB and the CRTC co-activators: sensors for hormonal and metabolic signals. Nature reviews Molecular cell biology. 2011; 12:141–151. DOI: 10.1038/nrm3072 [PubMed: 21346730]
22. Keeley MB, Busch J, Singh R, Abel T. TetR hybrid transcription factors report cell signaling and are inhibited by doxycycline. BioTechniques. 2005; 39:529–536. [PubMed: 16235565]
23. Ge H, et al. Generation of novel long-acting globular adiponectin molecules. Journal of molecular biology. 2010; 399:113–119. DOI: 10.1016/j.jmb.2010.03.062 [PubMed: 20382165]
24. Matthews DR, et al. Homeostasis model assessment: insulin resistance and beta-cell function from fasting plasma glucose and insulin concentrations in man. Diabetologia. 1985; 28:412–419. [PubMed: 3899825]
25. Alberti KG, Zimmet PZ. Definition, diagnosis and classification of diabetes mellitus and its complications. Part 1: diagnosis and classification of diabetes mellitus provisional report of a WHO consultation. Diabet Med. 1998; 15:539–553. DOI: 10.1002/(SICI)1096-9136(199807)15:7<539::AID-DIA668>3.0.CO;2-S [PubMed: 9686693]
26. Bornfeldt KE, Tabas I. Insulin resistance, hyperglycemia, and atherosclerosis. Cell metabolism. 2011; 14:575–585. DOI: 10.1016/j.cmet.2011.07.015 [PubMed: 22055501]
27. Weber W, Fussenegger M. Emerging biomedical applications of synthetic biology. Nature reviews Genetics. 2012; 13:21–35. DOI: 10.1038/nrg3094
28. Ruder WC, Lu T, Collins JJ. Synthetic biology moving into the clinic. Science. 2011; 333:1248–1252. DOI: 10.1126/science.1206843 [PubMed: 21885773]
29. Wu CY, Rupp LJ, Roybal KT, Lim WA. Synthetic biology approaches to engineer T cells. Curr Opin Immunol. 2015; 35:123–130. DOI: 10.1016/j.coi.2015.06.015 [PubMed: 26218616]
30. Heng BC, Aubel D, Fussenegger M. Prosthetic gene networks as an alternative to standard pharmacotherapies for metabolic disorders. Current opinion in biotechnology. 2015; 35:37–45. DOI: 10.1016/j.copbio.2015.01.010 [PubMed: 25679308]
31. Kojima R, Aubel D, Fussenegger M. Novel theranostic agents for next-generation personalized medicine: small molecules, nanoparticles, and engineered mammalian cells. Current opinion in chemical biology. 2015; 28:29–38. DOI: 10.1016/j.cbpa.2015.05.021 [PubMed: 26056952]
32. Okada-Iwabu M, et al. A small-molecule AdipoR agonist for type 2 diabetes and short life in obesity. Nature. 2013; 503:493–499. DOI: 10.1038/nature12656 [PubMed: 24172895]
33. Fussenegger M, et al. Streptogramin-based gene regulation systems for mammalian cells. Nature biotechnology. 2000; 18:1203–1208. DOI: 10.1038/81208
34. Trounson A, DeWitt ND. Pluripotent stem cells progressing to the clinic. Nature reviews Molecular cell biology. 2016; 17:194–200. DOI: 10.1038/nrm.2016.10 [PubMed: 26908143]
35. Lathuiliere A, Cosson S, Lutolf MP, Schneider BL, Aebischer P. A high-capacity cell macroencapsulation system supporting the long-term survival of genetically engineered allogeneic cells. Biomaterials. 2014; 35:779–791. DOI: 10.1016/j.biomaterials.2013.09.071 [PubMed: 24103654]
36. Simonsen JL, et al. Telomerase expression extends the proliferative life-span and maintains the osteogenic potential of human bone marrow stromal cells. Nature biotechnology. 2002; 20:592–596. DOI: 10.1038/nbt0602-592
37. Wieland M, Auslander D, Fussenegger M. Engineering of ribozyme-based riboswitches for mammalian cells. Methods. 2012; 56:351–357. DOI: 10.1016/j.ymeth.2012.01.005 [PubMed: 22305857]

38. Mates L, et al. Molecular evolution of a novel hyperactive Sleeping Beauty transposase enables robust stable gene transfer in vertebrates. Nature genetics. 2009; 41:753–761. DOI: 10.1038/ng.343 [PubMed: 19412179]

39. Schlatter S, Rimann M, Kelm J, Fussenegger M. SAMY, a novel mammalian reporter gene derived from Bacillus stearothermophilus alpha-amylase. Gene. 2002; 282:19–31. [PubMed: 11814674]

40. Weber W, et al. Gas-inducible transgene expression in mammalian cells and mice. Nature biotechnology. 2004; 22:1440–1444. DOI: 10.1038/nbt1021

41. Kemmer C, et al. A designer network coordinating bovine artificial insemination by ovulation-triggered release of implanted sperms. Journal of controlled release : official journal of the Controlled Release Society. 2011; 150:23–29. DOI: 10.1016/j.jconrel.2010.11.016 [PubMed: 21108977]

42. Folcher M, Xie M, Spinnler A, Fussenegger M. Synthetic mammalian trigger-controlled bipartite transcription factors. Nucleic acids research. 2013; 41:e134.doi: 10.1093/nar/gkt405 [PubMed: 23685433]

Europe PMC Funders Author Manuscripts

Europe PMC Funders Author Manuscripts

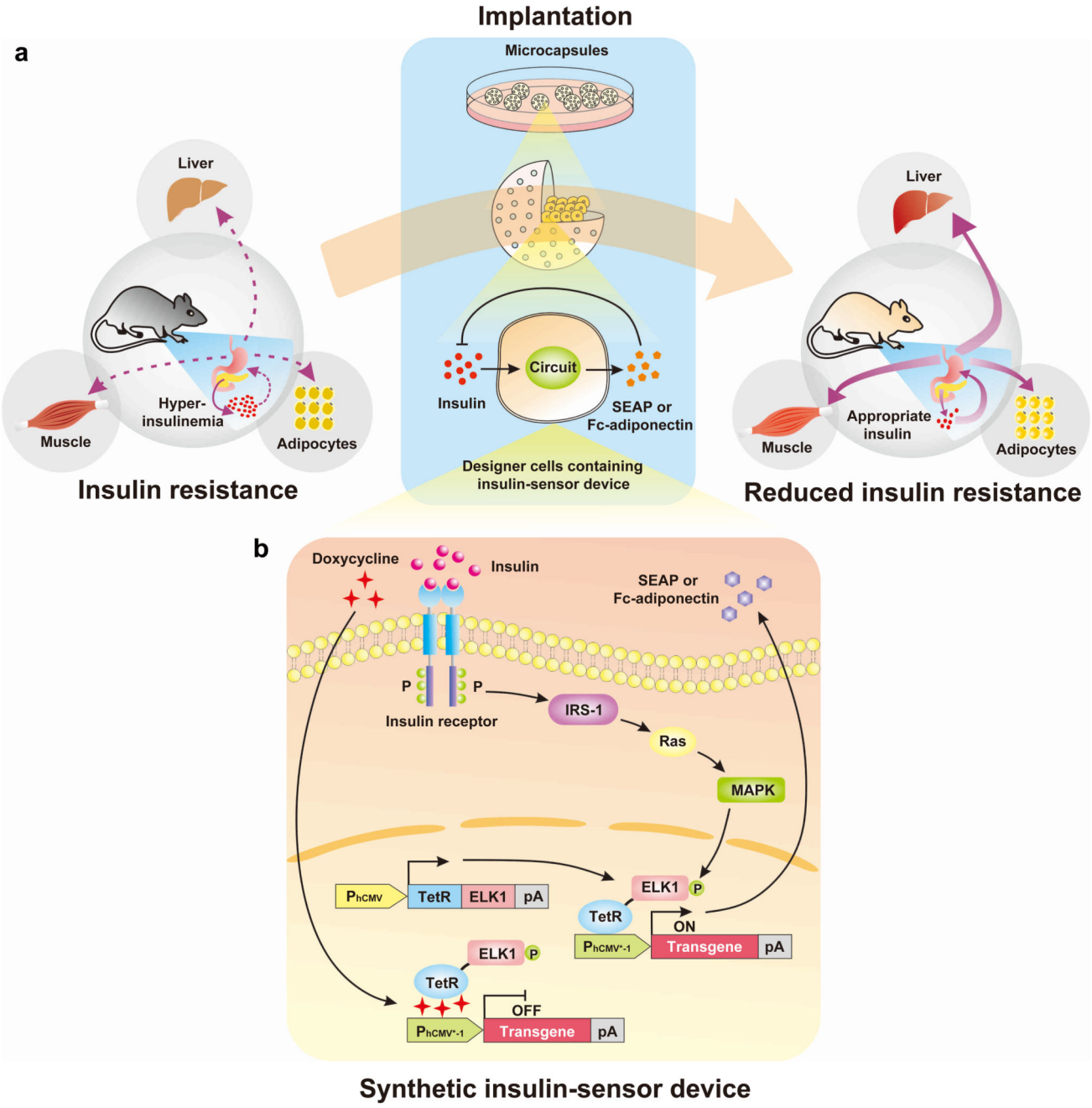

Figure 1. Synthetic insulin-sensitizing designer circuit for the treatment of insulin resistance.

(a) Functional and therapeutic features. Insulin resistance is characterized by the insensitivity of liver, muscle and adipocytes to blood insulin levels, which prevents cellular glucose uptake and leads to hyperinsulinaemia. The designer circuit quantifies blood insulin levels, detects hyperinsulinaemia and triggers dose-dependent adiponectin expression, which restores insulin sensitivity and attenuates the insulin-resistance syndrome. **(b)** Synthetic insulin-sensitizing designer cascade. The binding of insulin to the tyrosine kinase family human insulin receptor (IR) triggers autophosphorylation on multiple tyrosine residues in

Europe PMC Funders Author Manuscripts

the IR, leading to the phosphorylation of cellular proteins such as insulin receptor substrate 1 (IRS-1). Upon tyrosine phosphorylation, these proteins interact with signaling molecules through their SH_2 domains, resulting in subequent activation of Ras (a GTPase) and mitogen-activated protein kinase (MAPK). The activated MAPK enters the nucleus and phosphorylates the synthetic hybrid transcription factor, TetR-ELK1, consisting of the doxycycline-responsive DNA-binding Tet repressor (TetR) fused to the regulated activation domain of the transcription factor, ELK1, which is driven by the constitutive human cytomegalovirus immediate early promoter (P_{hCMV}). In the basal state, TetR-ELK1, is able to bind to $P_{hCMV*-1}$, a chimeric promoter containing a TetR-specific heptameric operator module ($tetO_7$) linked to a minimal version of P_{hCMV} ($P_{hCMVmin}$), but the ELK1 domain remains inactive. Only the phosphorylation of TetR-ELK1's ELK1 domain by upstream MAPK activity during cell signaling leads to $P_{hCMV*-1}$-driven expression of the desired transgene. The addition of doxycycline disrupts the interaction between TetR-ELK1's TetR domain and the $tetO_7$ operator of $P_{hCMV*-1}$, preventing the hybrid transcription factor from mediating the transgene expression, regardless of its phosphorylation state. When set to produce a therapeutic protein such as adiponectin that is secreted into the bloodstream the designer cascade turns into a closed-loop prosthetic network that increases the sensitivity of liver, adipose and muscle tissues to insulin which attenuates insulin release by pancreatic beta cells and reverses the insulin resistance syndrome.

Europe PMC Funders Author Manuscripts

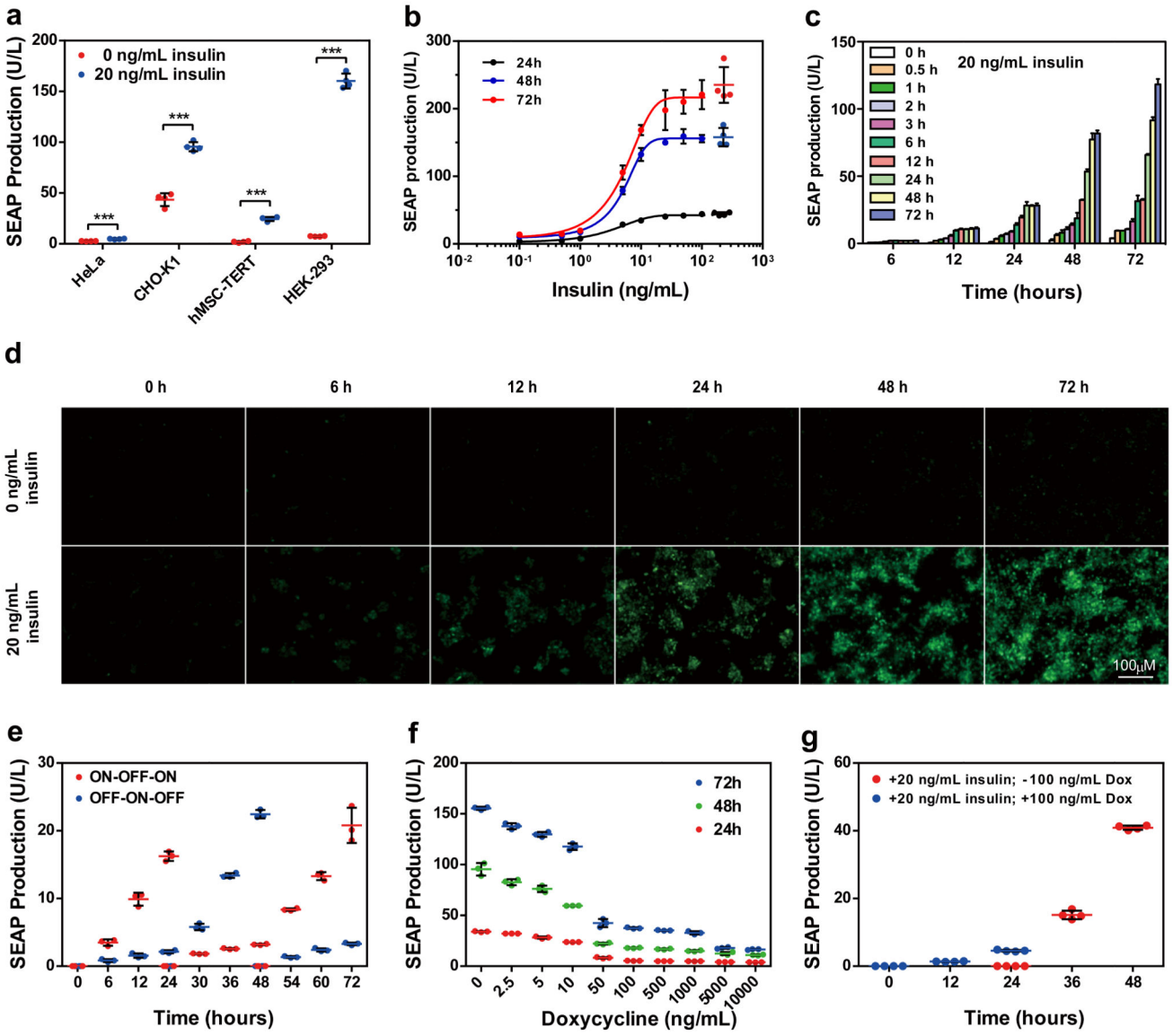

Figure 2. Synthetic insulin-inducible mammalian sensor circuit.

(**a**) Insulin-inducible transgene expression in different mammalian cell lines. Insulin-triggered SEAP expression by HeLa, CHO-K1, hMSC-TERT and HEK-293 cells 72 h after cotransfection with pIR (P_{hCMV}-IR-pA), pTetR-ELK1 (P_{hCMV}-TetR-ELK1-pA) and pMF111 ($P_{hCMV*-1}$-SEAP-pA) at a ratio of 1:1:1. The data represent the mean ± SD; n=4 independent experiments, statistical analysis using a two-tailed Student's *t*-test, ***$P <$ 0.001 vs. control. (**b**) The SEAP expression kinetics of HEK-293 cells cotransfected with pIR, pTetR-ELK1 and pMF111 at a ratio of 1:1:1 and cultivated for 24, 48 and 72 h in the presence or absence of different concentrations of insulin. For points with error bars comparable to the size of the symbols, only mean ± SD is displayed instead of individual points; n=4 independent experiments. (**c**) SEAP expression profiles of pIR-/pTetR-ELK1-/pMF111-cotransfected HEK-293 cells cultivated for different periods of time in the presence of 20 ng/mL insulin. The data represent the mean ± SD; n=3 independent experiments. (**d**)

Europe PMC Funders Author Manuscripts

Fluorescence micrographs profiling EYFP expression by HEK-293 cells cotransfected with pIR, pTetR-ELK1 and pHY74 ($P_{hCMV*-1}$-EYFP-pA) and cultivated for 72 h in the presence or absence of 20 ng/mL insulin. (**e**) Reversibility of insulin-triggered SEAP expression in HEK-293 cells. pIR-/pTetR-ELK1-/pMF111-transgenic HEK-293 cells were cultivated for 72 h while alternating the insulin status of the culture (20 ng/mL, ON; 0 ng/mL, OFF) at 24 h and 48 h. The data represent the mean ± SD; n=3 independent experiments. (**f**) The inhibition of insulin-triggered SEAP expression by doxycycline in HEK-293 cells. pIR-/pTetR-ELK1-/pMF111-transgenic HEK-293 cells were cultivated in the presence of 20 ng/mL insulin and different concentrations of doxycycline. The data represent the mean ± SD; n=3 independent experiments. (**g**) Reversibility of doxycycline-triggered SEAP expression in HEK-293 cells. pIR-/pTetR-ELK1-/pMF111-transgenic HEK-293 cells were cultivated in the presence of 20 ng/mL insulin and 100 ng/mL doxycycline for the first 24 h and in the presence of 20 ng/mL insulin and absence of 100 ng/mL doxycycline for the following 24 h. Every 24 hours, the culture medium was exchanged, and the SEAP production was profiled for up to 48 h. The data represent the mean ± SD; n=4 independent experiments.

Europe PMC Funders Author Manuscripts

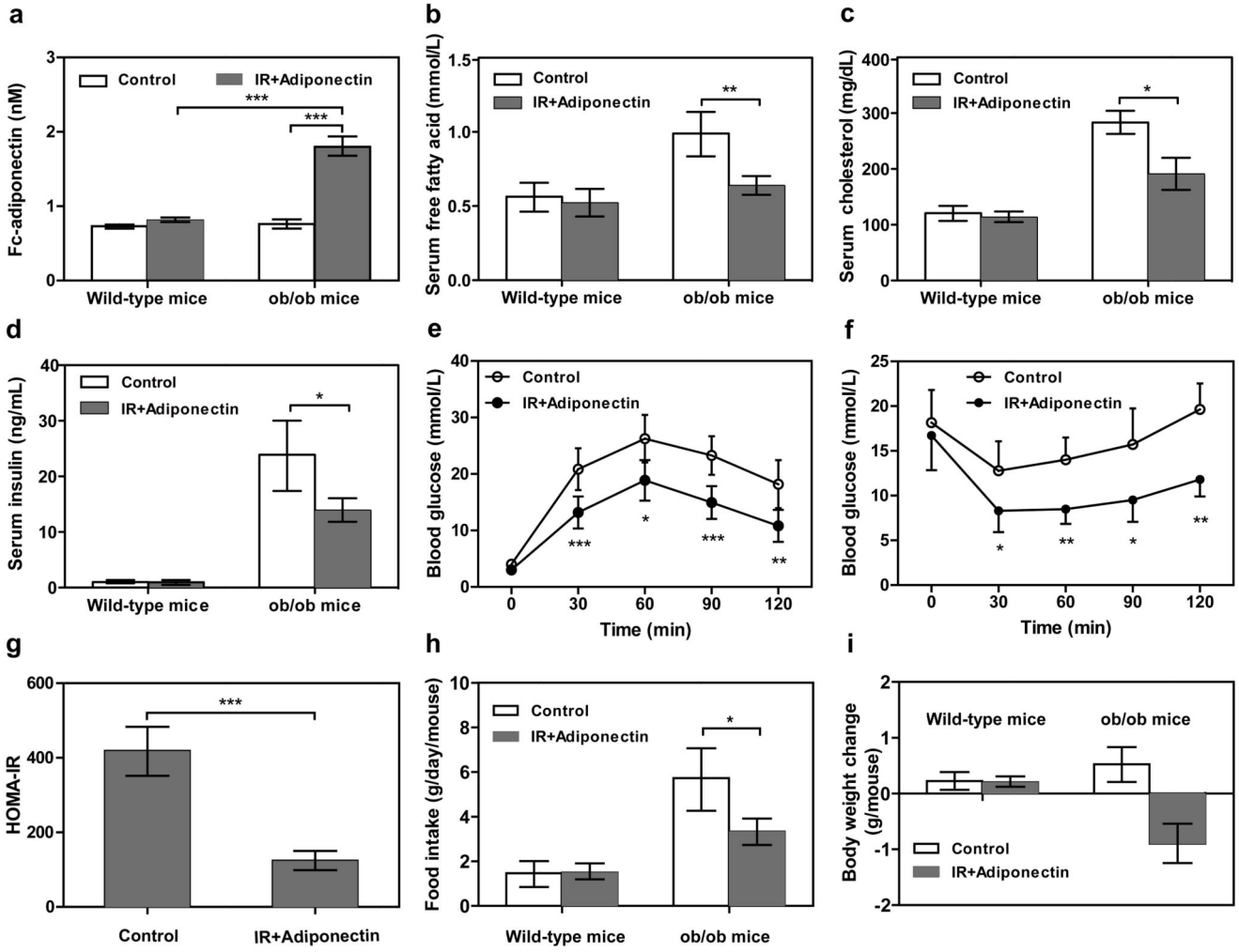

Figure 3. Self-sufficient insulin-sensor-based control of adiponectin expression in insulin-resistant ob/ob mice.

Animals were intraperitoneally implanted with $2x10^6$ encapsulated pIR-/pTetR-ELK1-/pHY79-transgenic HEK-293 cells (200 cells/capsule). Control mice were intraperitoneally implanted with $2x10^6$ encapsulated pKZY73-/pTetR-ELK1-/pHY79-transgenic HEK-293 cells. After 48 hours of implantation, the serum levels of (**a**) transgenic Fc-adiponectin (human IgG-Fc-tagged single-chain globular adiponectin consisting of three tandem adiponectin modules fused to the IgG1-derived Fc fragment), (**b**) free fatty acids, (**c**) cholesterol and (**d**) insulin were profiled. (**e**) Glucose tolerance test and (**f**) insulin tolerance test were performed 24 hours after implantation (serum adiponectin levels: 1.56±0.23nM). **(g)** HOMA-IR levels of ob/ob mice were determined 48 h after implantation. (h) Food intake and (i) body-weight change were quantified 72h after implantation. N.D., not detectable. The data represent the mean ± SEM, statistical analysis using a two-tailed Student's *t*-test, n=8 mice per group. $*P < 0.05$, $**P<0.01$, $***P < 0.001$ vs. control.

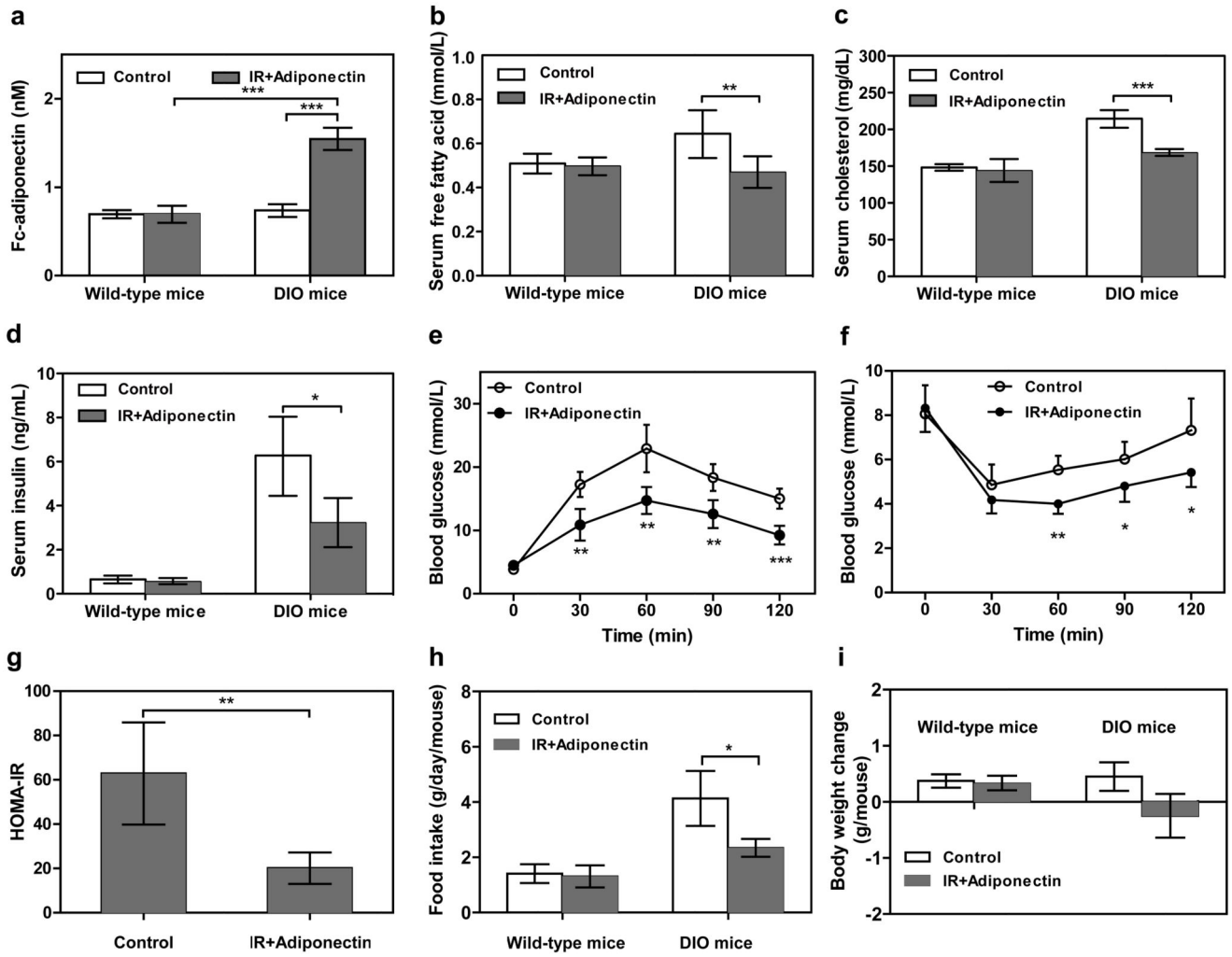

Figure 4. Self-sufficient insulin-sensor-based control of adiponectin expression in insulin-resistant DIO mice.

Mice fed for 10 weeks with normal caloric food (10 kcal% fat) or high-fat food (60 kcal% fat) were intraperitoneally implanted with $2x10^6$ encapsulated pIR-/pTetR-ELK1-/pHY79-transgenic HEK-293 cells (200 cells/capsule). Control mice were implanted with $2x10^6$ encapsulated pKZY73-/pTetR-ELK1-/pHY79-transgenic HEK-293 cells. Serum (**a**) adiponectin, (**b**) free fatty acid, (**c**) cholesterol and (**d**) insulin levels were profiled after 48 hours of implantation. (**e**) Glucose tolerance test and (**f**) insulin tolerance test were performed 24 hours after implantation (serum adiponectin levels: 1.38±0.18nM). **(g)** HOMA-IR levels of DIO mice were determined 48 h after implantation. (**h**) Food intake and (**i**) body-weight change were quantified 72h after implantation. N.D., not detectable. The data represent the mean ± SEM, statistical analysis using a two-tailed Student's *t*-test, n=8 mice per group. $*P < 0.05$, $**P<0.01$, $***P < 0.001$ vs. control.

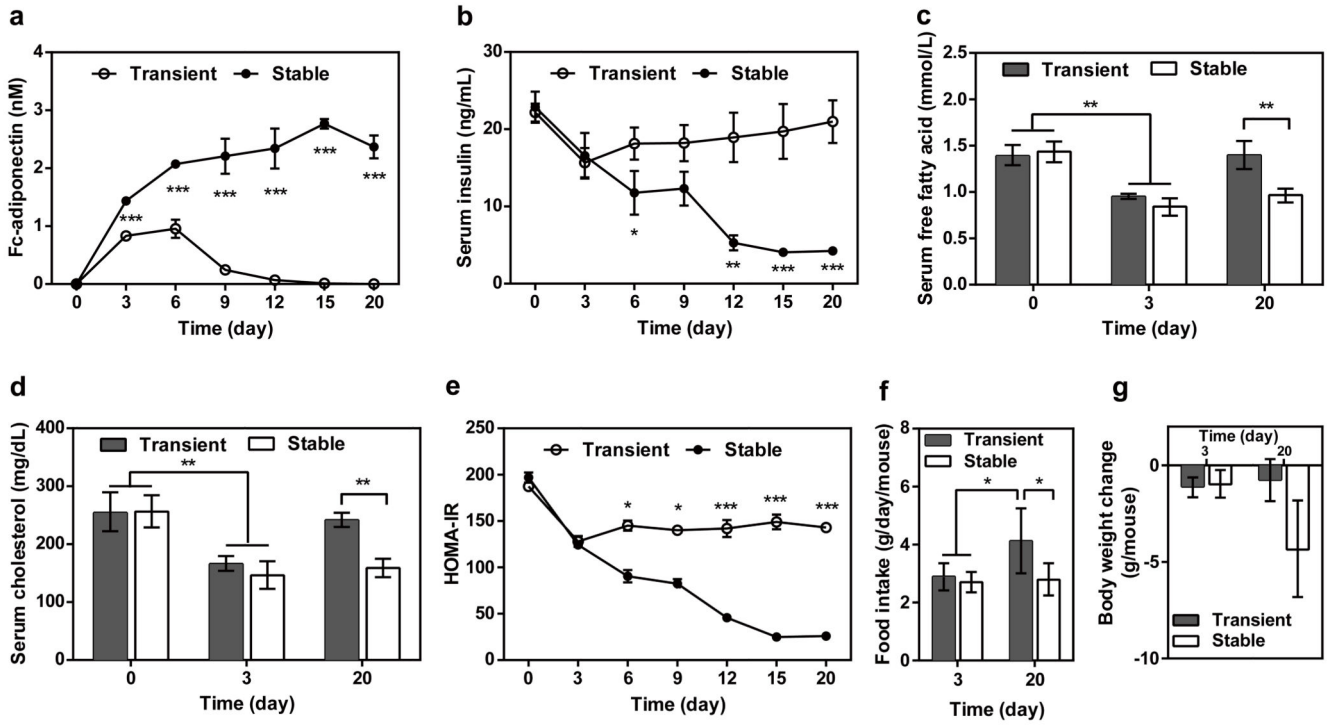

Figure 5. Long-term therapeutic efficacy of insulin-triggered adiponectin expression in insulin-resistant ob/ob mice.

Animals were intraperitoneally implanted with $2x10^6$ encapsulated $HEK_{IR\text{-}Adipo}$ cells (200 cells/capsule). Control animals received $2x10^6$ encapsulated pIR-/pTetR-ELK1-/pHY79-transgenic HEK-293 cells. Serum (**a**) adiponectin, (**b**) insulin (**c**) free fatty acid, and (**d**) cholesterol and (**e**) HOMA-IR values were determined for 20 days. (**f**) Food intake and (**g**) body-weight change were quantified on days 3 and 20. The data represent the mean ± SEM, statistical analysis using a two-tailed Student's *t*-test, n=8 mice per group. $*P < 0.05$, $**P<0.01$, $***P < 0.001$ vs. control.

Europe PMC Funders Author Manuscripts

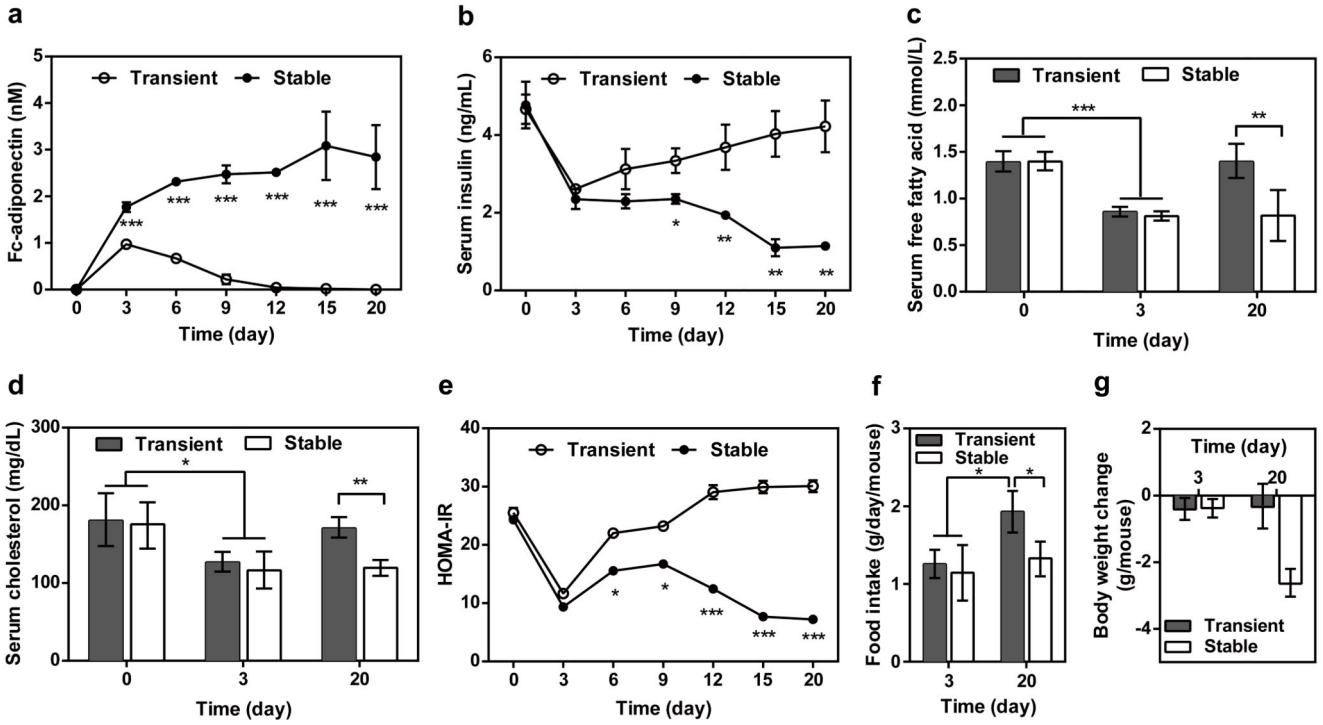

Figure 6. Long-term therapeutic efficacy of insulin-triggered adiponectin expression in insulin-resistant DIO mice.

Animals were intraperitoneally implanted with $2x10^6$ encapsulated $HEK_{IR\text{-}Adipo}$ cells (200 cells/capsule). Control mice received $2x10^6$ encapsulated pIR-/pTetR-ELK1-/pHY79-transgenic HEK-293 cells.Serum (**a**) adiponectin, (**b**) insulin (**c**) free fatty acid, and (**d**) cholesterol and (**e**) HOMA-IR values were determined for 20 days. (**f**) Food intake and (**g**) body-weight change were quantified on days 3 and 20. The data represent the mean ± SEM, statistical analysis using a two-tailed Student's *t*-test, n=8 mice per group. $*P < 0.05$, $**P<0.01$, $***P < 0.001$ vs. control.

Europe PMC Funders Author Manuscripts